

Biological Characteristics of Human-Urine-Derived Stem Cells: Potential for Cell-Based Therapy in Neurology

Jun-Jie Guan, MD, PhD,^{1,2,*} Xin Niu, MD,^{1,2,*} Fei-Xiang Gong, MD,³ Bin Hu, MD,² Shang-Chun Guo, MD,² Yuan-Lei Lou, MD,³ Chang-Qing Zhang, MD, PhD,^{1,2} Zhi-Feng Deng, MD, PhD,^{3,4} and Yang Wang, PhD^{1,2}

Stem cells in human urine have gained attention in recent years; however, urine-derived stem cells (USCs) are far from being well elucidated. In this study, we compared the biological characteristics of USCs with adipose-derived stem cells (ASCs) and investigated whether USCs could serve as a potential cell source for neural tissue engineering. USCs were isolated from voided urine with a modified culture medium. Through a series of experiments, we examined the growth rate, surface antigens, and differentiation potential of USCs, and compared them with ASCs. USCs showed robust proliferation ability. After serial propagation, USCs retained normal karyotypes. Cell surface antigen expression of USCs was similar to ASCs. With lineage-specific induction factors, USCs could differentiate toward the osteogenic, chondrogenic, adipogenic, and neurogenic lineages. To assess the ability of USCs to survive, differentiate, and migrate, they were seeded onto hydrogel scaffold and transplanted into rat brain. The results showed that USCs were able to survive in the lesion site, migrate to other areas, and express proteins that were associated with neural phenotypes. The results of our study demonstrate that USCs possess similar biological characteristics with ASCs and have multilineage differentiation potential. Moreover USCs can differentiate to neuron-like cells in rat brain. The present study shows that USCs are a promising cell source for tissue engineering and regenerative medicine.

Introduction

STEM CELLS can self-renew and generate committed cells in special tissues. Thus, stem cells play a critical role in tissue repair and regeneration. Recently a stem cell population was isolated from voided urine, which exhibits self-renew and multilineage differentiation ability. Under certain growth factors, urine-derived stem cells (USCs) can differentiate into urothelium, smooth muscle, and endothelium.^{1,2} Some studies have attempted to use USCs for tissue engineering and cytotrophy. In one study, USCs were implanted in bacterial cellulose to regenerate urinary conduit; the results showed that the composition formed a multilayered urothelium.³ Wu *et al.* isolated USCs and seeded them onto a porous scaffold, and after implanted into athymic mice, the composition showed a similar structure to native urinary tract tissue.⁴ Very recently Bharadwaj *et al.* identified a subpopulation of USCs with the capacity of multilineage differentiation potential.⁵ Adipose tissue also

contains multilineage differentiation cells (adipose-derived stem cells [ASCs]) and ASCs have been widely used in laboratory research and therapeutic applications.⁶⁻⁸ As an alternative and promising source for cellular therapy, whether USCs have the same biological characteristic with ASCs is unknown.

Brain trauma or stroke often results in cavity formation within brain tissue. How to fill the cavity with functional neuron is a big challenge for neuron regeneration. Neural tissue engineering provides a potential solution for neural diseases.⁹ However, there are still limitations in its application such as shortage of a suitable cell source. In 2009, U.S. Food and Drug Administration approved the first clinical trial of embryonic stem cells to treat spinal cord injury.¹⁰ However, in 2012, the entire program was halted due to financial concerns.¹¹ Previous study demonstrated that ASCs may serve as a promising stem cell source for neural tissue engineering.¹² But the source of ASCs is limited and the procedure of isolation is invasive. Therefore,

¹Department of Orthopedic Surgery, Shanghai Sixth People's Hospital, Shanghai Jiaotong University, Shanghai, China.

²Institute of Microsurgery on Extremities, Shanghai Sixth People's Hospital, Shanghai, China.

³Department of Neurosurgery, The Second Affiliated Hospital of Nanchang University, Nanchang, China.

⁴Department of Neurosurgery, Shanghai Sixth People's Hospital, Shanghai Jiaotong University, Shanghai, China.

*These authors contributed equally to this work.

a new source of stem cells that can be safely and efficiently obtained is still highly demanded. USC's can be harvested in a safe and low-cost method. Meanwhile, USC's were isolated from voided urine, which promises the large amount of supplement. Up to now, it has not been investigated whether USC's can be applied in neural regeneration.

Neural tissue engineering has a specific requirement for scaffold due to the unique biological properties of brain. As hydrogel scaffolds can provide favorable cellular microenvironments to support neural regeneration, they have been used extensively in neural tissue engineering.¹³ Besides, hydrogel can potentially conformally fill irregular neural tissue defects.¹⁴ BeaverNano™ hydrogel scaffold is composed of polypeptide biological nanomaterial. Polypeptides are widely utilized scaffold materials for its unique properties, such as biodegradability, biocompatibility, and potential to be fabricated in appropriate forms to regenerate injured tissues.^{15,16}

We investigated the intrinsic properties of USC's and compared their biological characteristics with ASC's. Further, USC's were seeded on BeaverNano hydrogel scaffold and transplanted into rat brain to explore the therapeutic application of USC's in neuronal regeneration. We demonstrated that USC's have similar biological characteristics with ASC's and could be an alternative cell source for neural tissue engineering.

Materials and Methods

Isolation and proliferation of USC's and ASC's

This study was carried out in accordance with the principles of the Helsinki Declaration, and was approved by the Ethical Review Board of Shanghai Sixth People's Hospital affiliated to Jiaotong University. Urine samples were obtained from eight healthy men with a mean age of 25 years (age range, 22–28 years). Human adipose tissue was obtained from four patients who carried out liposuction. The written informed consents were obtained from all study participants.

For isolation and proliferation of USC's, penicillin and streptomycin were added in the fresh urine samples (200 mL) as recommended concentrations to minimize the contamination. After the urine sample was centrifuged at 400 *g* for 10 min at room temperature, the supernatant was discarded and the sediment was washed with phosphate-buffered saline (PBS). Cells were washed and centrifuged again. Then, the sediment was resuspended with Dulbecco's modified Eagle's medium (DMEM) culture media supplemented with 2% (v/v) fetal bovine serum (FBS; Gibco, Invitrogen Corp.), 10 ng/mL human epidermal growth factor (hEGF; Peprotech), 2 ng/mL platelet-derived growth factor (PDGF; Millipore), 1 ng/mL transforming growth factor- β (TGF- β ; Peprotech), 2 ng/mL basic fibroblast growth factor (bFGF; Sigma-Aldrich), 0.5 μ M cortisol (Sigma-Aldrich), 25 μ g/mL insulin (Humulin), 20 μ g/mL transferrin, 549 ng/mL adrenaline, 50 ng/mL triiodothyronine, L-glutamine, and antibiotics. The cell suspension was plated into gelatin-coated 24-well plate and incubated at 37°C in a humidified atmosphere of 5% CO₂. The medium was first changed after 7 days of culture and the nonadherent cells were removed by washing with PBS. The colonies derived from single cells were marked. The culture medium was refreshed twice a week thereafter. When the cells became near

80% confluence, they were passaged with 0.25% trypsin containing 1 mM EDTA.

For isolation and proliferation of ASC's, fresh adipose tissue was washed extensively with PBS and minced into <1 mm³ pieces with sterile scissors. After that, the tissue was digested with sterile-filtered collagenase (Sigma-Aldrich) for 60 min at 37°C with intermittent shaking. Then, the enzyme was inactivated with DMEM containing 10% FBS and centrifuged at 250 *g* for 10 min at room temperature. The lipid layer and PBS supernatant were separated from the stromal vascular fraction (SVF). The SVF was resuspended in DMEM/10% FBS and plated in T-25 cm² culture flask. The cells were cultured in a 5% CO₂/humidified incubator maintained at 37°C. The medium was first changed after 96 h of the initial plating and afterward twice a week. When cells became 80%–90% confluent, they were passaged by treatment with 0.25% trypsin containing 1 mM EDTA.

For both USC's and ASC's, the cells at the passages 4 were plated to obtain standard prototype growth curves using CCK-8 according to the manufacturer's instruction (Dojindo Laboratories). The cells were seeded into a 96-well plate at 5000 cells/well with 100 μ L culture medium. The cell proliferation assay was performed on days 1, 2, 3, 4, 5, 6, and 7. A 10- μ L of CCK-8 solution was added to each well and then the plates were incubated at 37°C for 3 h. At the end of the incubation, the absorbance at 450 nm was measured with a Microplate Reader (iMark™; Bio-Rad). All experiments were done in triplicate and repeated at three independent times.

Flow cytometry and karyotype analysis

The cultured cells at passages 4 were detached from the flask using trypsin-EDTA and were incubated with 3% BSA for 30 min to block nonspecific antigens. After the fixation, single-cell suspensions were incubated with 0.5% Triton X-100 (Sigma-Aldrich) for 5 min at 4°C. The cells were then incubated with the following monoclonal antibodies: CD34-APC BD (No. 560940), CD133-PE Miltenyi (No. 130-080-801), CD45-PE BD (No. 560976), CD29-PE BD (No. 561795), CD44-FITC BD (No. 560977), CD73-PE BD (No. 561014), CD90-FITC BD (No. 561969), CD105 Abcam (No. ab114052), and HLA-DR-PE BD (No. 560943). The cells were washed to remove unbound antibody and then similarly processed with the secondary antibody when needed. Surface antigens were analyzed using Guava easyCyte™.

Karyotype analysis was performed on USC's to test their chromosomal stability. The cells at the passage 15 were subjected to metaphase mitotic arrest using 20 μ g/mL colchicines for 4–5 h in a 37°C incubator. The cells were treated with 0.075 M hypotonic potassium for 15 min at 37°C and fixed with 3:1 methanol-to-acetic acid fixative. Metaphase spreads on the cleaned slides were digested using trypsin and followed by Giemsa stain to visualize G-banding. Images were acquired using a microscope (TY9648; Leica).

Multilineage differentiation potential of USC's and ASC's: in vitro studies

Osteogenic induction. The cultured USC's and ASC's at the passage 4 were grown to 80% confluence and then

incubated with osteogenic induction media (Cyagen Biosciences). At 21 days of the induction, Alizarin Red S and von Kossa staining were utilized to detect calcified matrix deposition. After the cells were observed under an inverted optical microscope, the Alizarin Red S was eluted by adding 10% cetylpyridinium chloride for 1 h. The absorbance of the collected liquid was read on the Microplate reader at the wavelength of 550 nm (iMark; Bio-Rad). The primary antibodies, including mouse anti-human Osteocalcin (1:100; Abcam) and mouse anti-human Runx2 (10 μ g/mL; Abcam), were added to the cells followed by incubation overnight at 4°C. A secondary goat anti-mouse Alexa Fluor 594 (1:250; Invitrogen) was added and incubated in the dark for 1 h at 37°C. The cell nucleus was counterstained with DAPI for 5 min and then washed with PBS. The fluorescent-stained cells were imaged by a fluorescence microscope (MZFL III; Leica).

Adipogenic induction. The cultured USCs and ASCs were grown to 90% confluence and then incubated with adipogenic medium (Gibco, Invitrogen Corp.). The culture medium was changed every 3 days. The control cells were cultured with original medium without induction medium. After 14 days of the induction, the cells were fixed in 4% paraformaldehyde (PFA) for 30 min at room temperature and stained with Oil Red O for 10 min. Quantification of lipid accumulation was achieved by extracting Oil Red O and then measured the absorbance value at 510 nm using the Microplate Reader (iMark; Bio-Rad).

Chondrogenic induction. Chondrogenic differentiation of USCs and ASCs was induced using a pellet culture technique. Briefly, 1×10^6 cells were centrifuged in a 15-mL centrifugal tube and the cells formed a pellet at the bottom of the tube. Chondrogenic medium was gently added to the pellet (Gibco, Invitrogen Corp.). After the induction for 4 weeks, the pellets were fixed in 4% PFA and embedded in optimum cutting temperature compound. The cryosections at 10- μ m thickness were stained with hematoxylin and eosin (H&E). Toluidine blue and Safranin-O were used to show extracellular matrix sulfated proteoglycans. Masson Trichrome staining was employed to display the collagen fibers. Anti-type II collagen (1:100; Millipore) and anti-Sox9 (1:100; Abcam) antibodies were incubated for 2 h, rinsed twice with PBS, and then stained with anti-mouse Alexa Fluor 594 IgG (1:200; Jackson) or goat anti-mouse Alexa Fluor 488 IgG (1:200; Life Technologies). The nucleus was stained with DAPI. All the stained cells were observed under the fluorescence microscope (MZFL III; Leica).

Neural induction. The *in vitro* differentiation of USCs into neural progenitor cells was carried out according to the method as previously described with minor modifications.¹⁷ The USCs were seeded onto the plate coated with polystyrene. When the plate cells are 30% to 50% confluency, the neural induction medium was added. The neural differentiation medium consisted of DMEM/F12 medium supplemented with 20 ng/mL hEGF (Peprotech), 40 ng/mL bFGF (Applied StemCell), 2% B27, 1% nonessential amino acid, 1% L-glutamine, and 1% insulin-transferrin-selenite (ITS). The culture medium was changed every 3 days. After 12 days of the induction, the mRNA expression of neuronal markers Nestin, Sox2, and β -III-tubulin was examined. The

cells were stained with mouse anti-Nestin (1:100; Abcam) and mouse anti-Sox2 (1:50; Cell Signaling Technology) antibodies, followed by goat anti-mouse Alexa Fluor 594 IgG(H+L) (1:150; Jackson) or goat anti-mouse Alexa Fluor 488 IgG(H+L) (1:100; Life Technologies) antibody.

Quantitative reverse-transcriptase–polymerase chain reaction

After osteogenic, adipogenic, and neurogenic induction, cellular RNA samples were extracted with Trizol Reagent (Invitrogen).¹⁸ One microgram of RNA was transcribed using reverse-transcriptase–polymerase chain reaction (RT-PCR) kit (Takara). RT-PCR was performed on a 7900 Real-Time PCR System using TaqMan Universal PCR Master Mix (Roche) according to the protocols provided by the manufacturers. Primer sequences used for RT-PCR are shown in Table 1. The expression level of glyceraldehyde-3-phosphate dehydrogenase (GAPDH) was used as the endogenous control.

USCs for neural tissue engineering: in vivo study

BeaverNano hydrogel scaffolds. The scaffolds were purchased from Cyagen Biosciences.

Cell transfection. The USCs at the passage 4 were transfected with green fluorescent protein (GFP) using GFP lentivirus according to manufacturer's instruction (Genechem). The cells were grown in 25 cm² culture flask in a density of 5×10^5 /mL. Then, the cells were infected with lentivirus containing GFP gene in the presence of a polybrene solution. After 4 h, the lentivirus-containing medium was replaced with the initial medium. The infected cells were placed at 37°C in a 5% CO₂ incubator for 24–48 h.

Animal model. SD rats at 8 weeks old were used for the transplantation of USCs. The animal model of the brain lesion was established as previously described.¹⁹ After the rat was anesthetized, a 5-mm-diameter craniotomy was performed under sterile conditions and 50 mm³ motor cortical tissues were removed by the resection.

Cell transplantation. USCs were digested with trypsin and resuspended in 10% sucrose solution. Then, we gently mixed the nonionic cell suspension with an equal volume of hydrogel. After that, PBS was added into the mixture and the hydrogel begun the irreversible gelation process. One hundred milliliter of hydrogel containing 1×10^6 GFP-USCs was injected into the lesion site. After transplantation for 3 weeks, rats were anesthetized and perfused through the heart with 0.9% saline solution, followed by a fixative containing 4% PFA. The rat brains with hydrogel were carefully removed and fixed in 4% PFA at 4°C for overnight and then transferred to 20% and 30% sucrose to gradient dehydrate. The frozen coronal sections at 10- μ m thickness were prepared to test the expression of neural-lineage-specific markers. The sections were incubated with anti-GFAP (1:150; Cell Signaling Technology), anti- β -III-tubulin (1:50; Cell Signaling Technology), and anti-Nestin (1:100; Abcam), followed by goat anti-mouse Alexa Fluor 594 IgG(H+L) (1:150; Jackson).

TABLE 1. PRIMER SEQUENCES USED FOR RT-PCR IN THIS STUDY

Gene	Primer sequence (5'–3')	Amplification size (bp)	Ann. temp (°C)
Osteogenesis			
BMP-2	Forward GAGAAGGAGGAGGCAAAGAAA	161	56
	Reverse AGCAGCAACGCTAGAAGACAG		
RUNX2	Forward CCAACCCACGAATGCACTATC	71	58.9
	Reverse TAGTGAGTGGTGGCGGACATAC		
OCN	Forward CCCCCTCTAGCCTAGGACC	151	56.4
	Reverse ACCAGGTAATGCCAGTTTGC		
OPN	Forward CATGAGAATTGCAGTGTGTTGCT	121	56.7
	Reverse CTTGCAAGGGTCTGTGGGG		
ALP	Forward ACCACCACGAGAGTGAACCA	60	57.6
	Reverse CGTTGTCTGAGTACCAGTCCC		
LPL	Forward TGGAGGTACTTTTCAGCCAGGAT	81	60.0
	Reverse CGTGGGAGCACTTCACTAGCT		
Adipogenesis			
PPAR- γ	Forward CACAAGAACAGATCCAGTGGTTGCAG	179	64.8
	Reverse AATAATAAGGTGGAGATGCAGGCTCC		
aP2	Forward ATCTAGCAGACGGAAGTGAACCA	85	58
	Reverse TCTCGGACAGTATTCAGTTCGTTT		
Nestin	Forward GCCCTGACCACTCCAGTTTA	22	56.3
	Reverse GCCCTGACCACTCCAGTTTA		
Neurogenesis			
β -III-tubulin	Forward AGCAAGAACAGCAGCTAC TTC GT	80	58.6
	Reverse GATGAAGGTGGAGGACAT CTT GA		
Sox2	Forward GCCGAGTGGAACTTTTGTCTG	136	60.6
	Reverse GGCAGCGTGTACTTATCCTTCT		
NSE	Forward GGCTACACGGAAAAGATCGTTATT	24	58.7
	Reverse GAAGGATCAGTGGGAGACTTGAA		
GAPDH	Forward ATCCCATCACCATCTTCC	293	51.2
	Reverse GAGTCCCTCCACGATACCA		

GAPDH, glyceraldehyde-3-phosphate dehydrogenase; LPL, lipoprotein lipase; RT-PCR, reverse-transcriptase–polymerase chain reaction.

Statistical analysis

All data were calculated as mean \pm standard deviation. The differences between two groups were analyzed by using Student's *t*-test by SYSTAT version 16 (SPSS, Inc.). All the *p*-values were two-sided. The difference was considered significant if *p*-value < 0.05 .

Results

Cell morphology, growth curve, and karyotype analysis

To harvest a more purified adherent cells, we adopted a new mixed culture medium. Cell colonies in the USC-cultured plates were observed ~ 5 – 7 days after initial plating. The cells exhibited typical fibroblast-like morphology (Fig. 1a). The fibroblast-like cells had a robust proliferation capability and reached 80%–90% confluence after 10 days (Fig. 1b). After several passages USCs retained the elongated morphology (Fig. 1c). The primary ASCs adhered within 48 h after plating and showed spindle-shaped morphology (Fig. 1d). No microorganism contamination was observed in any culture plates.

We then compared the proliferation ability of USCs with ASCs. The USCs and ASCs displayed typical S-shape growth curves (Fig. 1e). CCK-8 assay showed that the cells were initially in the stationary phase during the first 1–2 days. Then the cells entered into rapid growth phase from

3rd to 4th day. After that, the cells maintained a slower growth trend started from the 5th to 6th day.

Further, we conducted karyotype tests to assess the safety of USCs. After prolonged cultivation *in vitro*, USCs still showed a normal karyotype (Fig. 1f). This result suggested that no tumorigenic phenotype was detected and USCs are safe for future application.

Cell surface marker expression in USCs and ASCs

Cell surface marker is a vital criterion to identify stem cells.²⁰ We used flow cytometer to compare the surface antigen expression of USCs and ASCs. Among the 10 predefined CD markers, both ASCs (Fig. 2A) and USCs (Fig. 2B) were positive for CD29, CD44, CD73, and CD90 antigen, and negative for CD31, CD34, CD45, CD133, CD309, and HLA-DR. USCs were weakly positive for CD105 while ASCs were strongly positive for CD105. The lack of CD34 and CD45 revealed that USCs were non-hematopoietic cells. Since CD133 represents the most specific marker for endothelial progenitor cells, the lack of CD133 may exclude the endothelial origin of these USCs.²¹

In vitro multilineage differentiation potential of USCs

The mesodermal differentiation potential, such as osteogenic, adipogenic, and chondrogenic cells, is a critical standard to define mesenchymal stem cell (MSC).²⁰ To explore

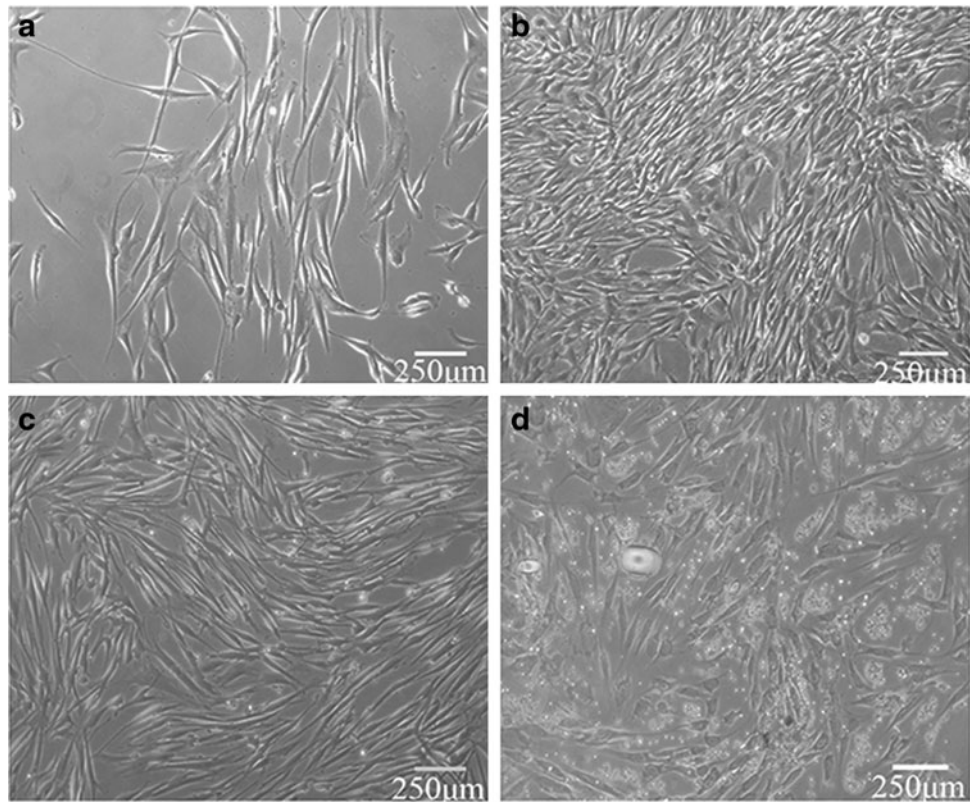
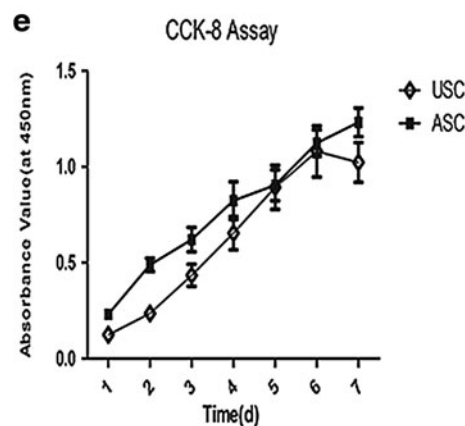


FIG. 1. Morphology and growth characteristics of urine-derived stem cells (USCs) and adipose-derived stem cells (ASCs). USCs showed fibroblast morphology (a). After 10-day culture period, USCs reached 90% confluence (b). USCs retained the fibroblast morphology after passages (c). The primary ASCs appeared spindle-shaped morphology (d). Growth curves of ASCs and USCs (e). Karyotype analysis showed that USCs had a normal size, shape, and number of chromosomes after repeated passages (f).



the multilineage differentiation potential of USCs, we analyzed the capacity of USCs to differentiate into osteoblast, adipocyte, and chondrocyte. Further, we also investigated the differentiation potential of USCs toward neural lineages.

Osteogenic differentiation. ASCs have demonstrated the capacity to differentiate into osteoblasts.²² Similar to ASCs, USCs also possess the ability to differentiate into osteoblasts. After 3 weeks of differentiation, Alizarin Red S and von Kossa staining showed direct evidence of amorphous calcium mineral deposits (USCs: Fig. 3a, c; ASCs: Fig. 3b, d). Immunofluorescence revealed that the expression of osteogenic-related proteins OCN and Runx2 was upregulated in induced USC group (Fig. 3e, f). The extent of matrix mineralization of USCs and ASCs was further evaluated by quantitating the Alizarin Red S staining

(Fig. 3g). Real-time PCR also showed that the expression of ALP, OCN, OPN, RUNX2, and BMP-2 was upregulated ($p < 0.05$; Fig. 3h).

Adipogenic differentiation. USCs and ASCs were adipogenic differentiated for 2 weeks. Before differentiation, USCs displayed fibroblast-like morphology (Fig. 4a). After 1 week of adipogenic induction, the morphology of differentiated USCs transformed into cuboid shape (Fig. 4b). The formation of tiny lipid droplets was observed at the end of the differentiation (Fig. 4c). Oil Red O staining demonstrated the formation of lipid droplets in cytoplasm in both induced USC and ASC groups (USCs: Fig. 4d; ASCs: Fig. 4e), whereas no lipid accumulation was observed in undifferentiated group (data not shown). With the increase of culture time, tiny lipid droplets merged into large lipid

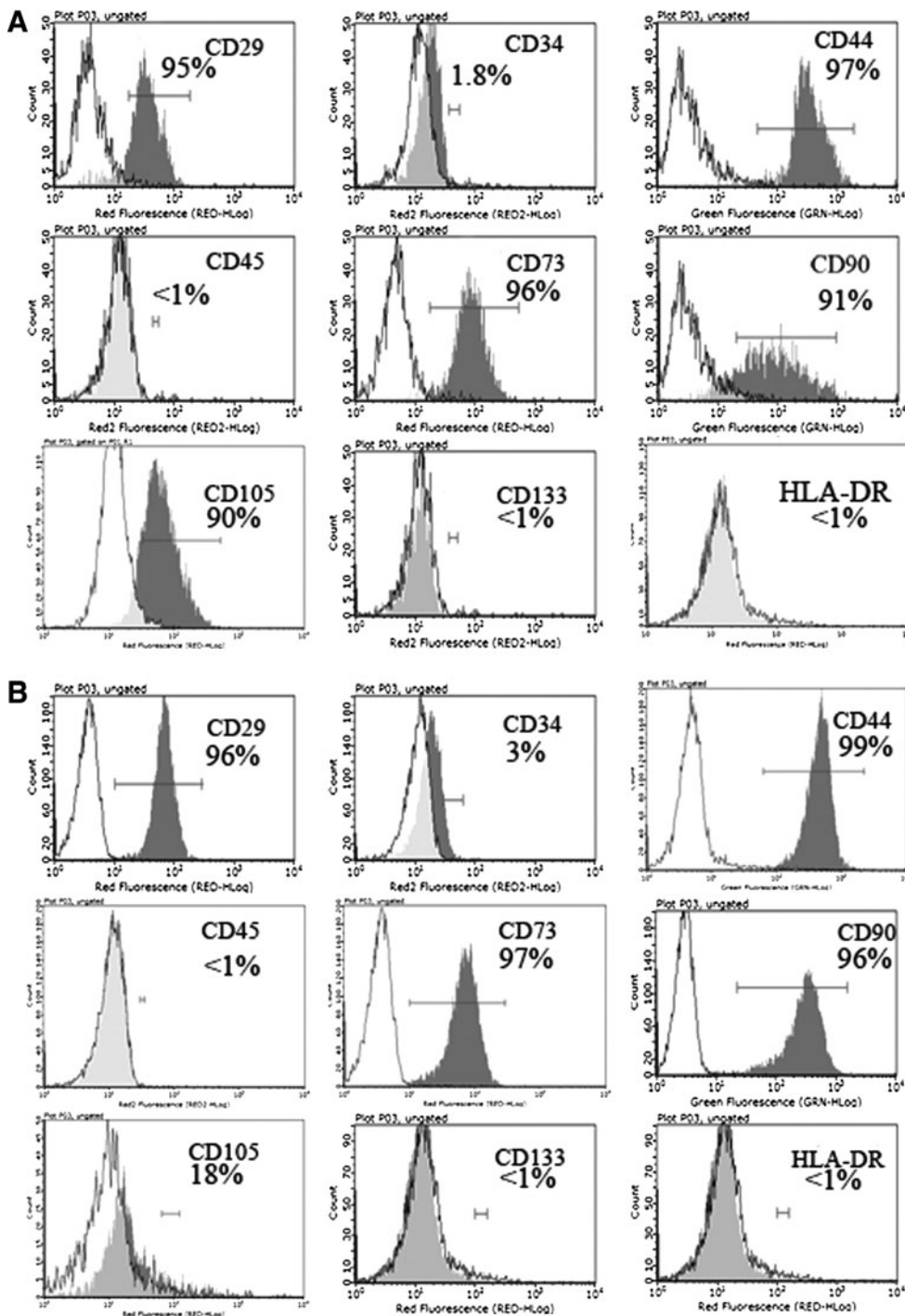


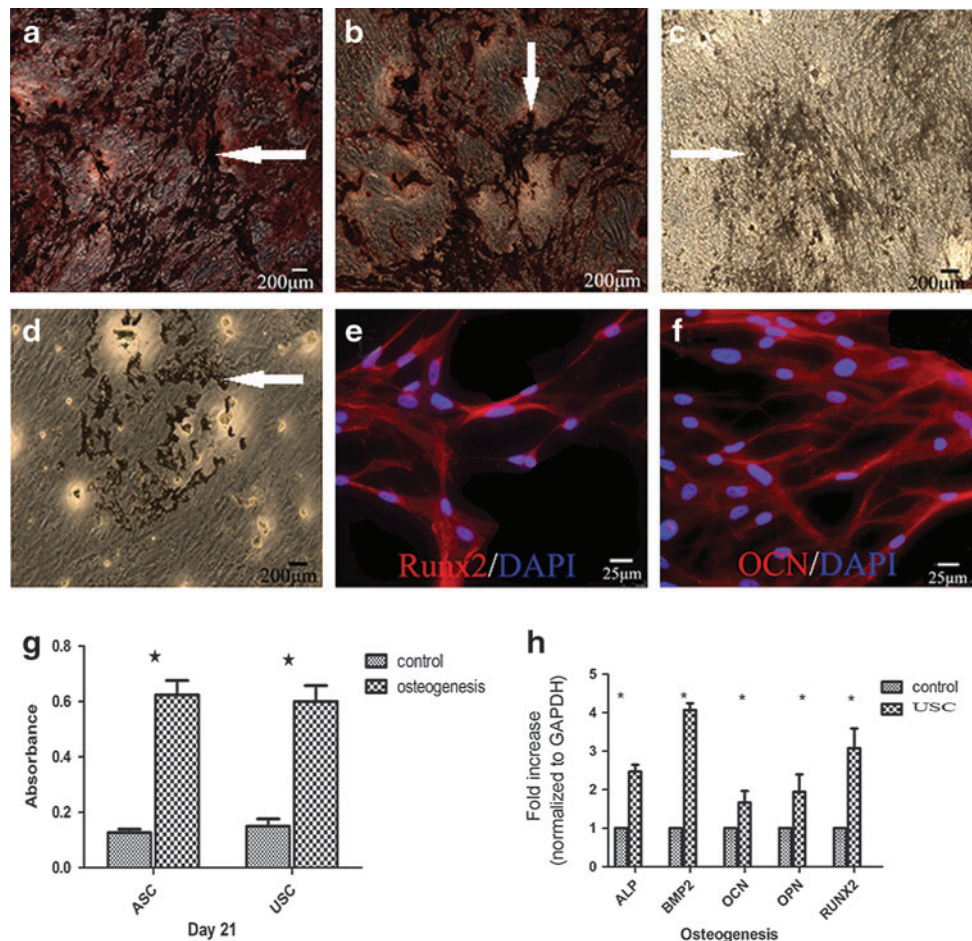
FIG. 2. ASCs and USCs were analyzed for surface markers. Black histogram represents the unlabelled control cells; gray histogram represents specific surface marker (**A:** ASCs; **B:** USCs).

droplets (Fig. 4f). Lipid quantification demonstrated that the two groups had no significant difference in lipid amount (Fig. 4g). An adipogenesis-related gene analysis demonstrated that the gene expression of PPAR- γ 2, lipoprotein lipase (LPL), and aP2 was upregulated in induced USCs (Fig. 4h).

Chondrogenic differentiation. After 4 weeks of chondrogenic differentiation, the pellet grew into spherical mass with shiny surfaces in both groups (USCs: Fig. 5a'; ASCs: Fig. 5b'). Toluidine blue staining revealed the presence of

polysaccharides and proteoglycans in both USC and ASC groups (USCs: Fig. 5a; ASCs: Fig. 5b). To further evaluate the chondrogenic differentiation potential of USCs, more special staining was performed. Morphological changes in cultured pellet cells were evaluated by H&E staining (Fig. 5c, d). Masson's trichrome and Safranin-O staining detected the presence of collagen and glycosaminoglycan (GAG) (Fig. 5e–g). Expression of the chondrogenic-related markers, such as Sox9 and collagen II, was detected by immunofluorescence (Fig. 5h, i). Results indicated that USCs undergone significant chondrogenic differentiation in pellet

FIG. 3. Osteogenic differentiation results of USCs and ASCs. Alizarin Red S staining and von Kossa staining were performed after 21 days of osteogenic induction (USCs: **a, c**; ASCs: **b, d**). The arrows indicate positive staining of Alizarin Red S and von Kossa staining. Immunofluorescence analysis of Runx2 and OCN expression in USCs after 21 days of induction (**e, f**). Quantitative analysis of the mineralization (**g**, ★ indicates significant difference of $p < 0.05$). The mRNA expression of osteogenesis-related genes (ALP, BMP-2, OCN, OPN, and Runx2) was quantitated in USCs after 21 days of induction (**h**). Data represent mean and standard deviation ($n = 3$). The single asterisks represent a significant differentiation between induction and control ($p < 0.05$). Panels (**a-d**) were taken under phase-contrast microscopy and panels (**e, f**) were taken under fluorescence microscopy. Color images available online at www.liebertpub.com/tea



culture system in the presence of chondrogenic induction medium.

Neural differentiation. USCs showed the potential to differentiate into neural progenitor cells *in vitro*. USCs displayed a fibroblast-like morphology before induction (Fig. 6a). After induced in neural induction medium, distinguished refractive cell bodies were observed at days 7 and 12 (Fig. 6b, c). The number of Sox2- and Nestin-positive cells was increased significantly, indicating that USCs differentiated into neural progenitor cells (Fig. 6d-f). Analysis of gene expression by RT-PCR showed that neuronal progenitor cell markers Nestin and Sox2 were significantly increased, while mature neuron marker β -III-tubulin was not upregulated (Fig. 6g).

Overall, the *in vitro* differentiation assays demonstrated that USCs have multilineage differentiation potential, which is similar with ASCs.

Survival and morphological characteristics of USCs after transplantation into rat brain

It is important for hydrogel scaffolds to have inter-connecting porous structures that allow efficient diffusion of nutrients and oxygen for cell growth. The SEM showed that the hydrogel scaffolds have sponge-like structures (Fig. 7a). Cell survival is a critical parameter to determine whether USCs can be potentially used for neural tissue engineering.

Therefore, we evaluated the survival of USCs by monitoring expression of GFP. After 3 weeks of transplantation, GFP-positive cells were found scattered in an area surrounding the lesion site (Fig. 7b). The morphology of GFP-positive cells had changed from being long spindle-like to an astrocyte-resembling morphology. Our results demonstrated that GFP-USCs could survive in rat brain after transplantation.

The migration and differentiation capacity of USCs in rat brain

After mixed with hydrogel scaffold, GFP-labeled USCs were injected into motor cortex. Three weeks after transplantation, GFP-positive cell bodies were detected in the hippocampus (Fig. 7c, d). To determine the differentiation status of USCs, we detected neurogenesis-related markers, including glial fibrillary acidic protein (GFAP), β -III-tubulin, and nestin. Even without neuronal differentiation before transplantation, transplanted GFP-positive cells were able to express β -III-tubulin, GFAP, and Nestin (Fig. 7f, i, l), indicating that they have been committed to neuronal lineages.

Discussion

In this study, we investigated the cellular properties of USCs and compared them with ASCs. We examined the ability of USCs to survive, migrate, and differentiate in rat

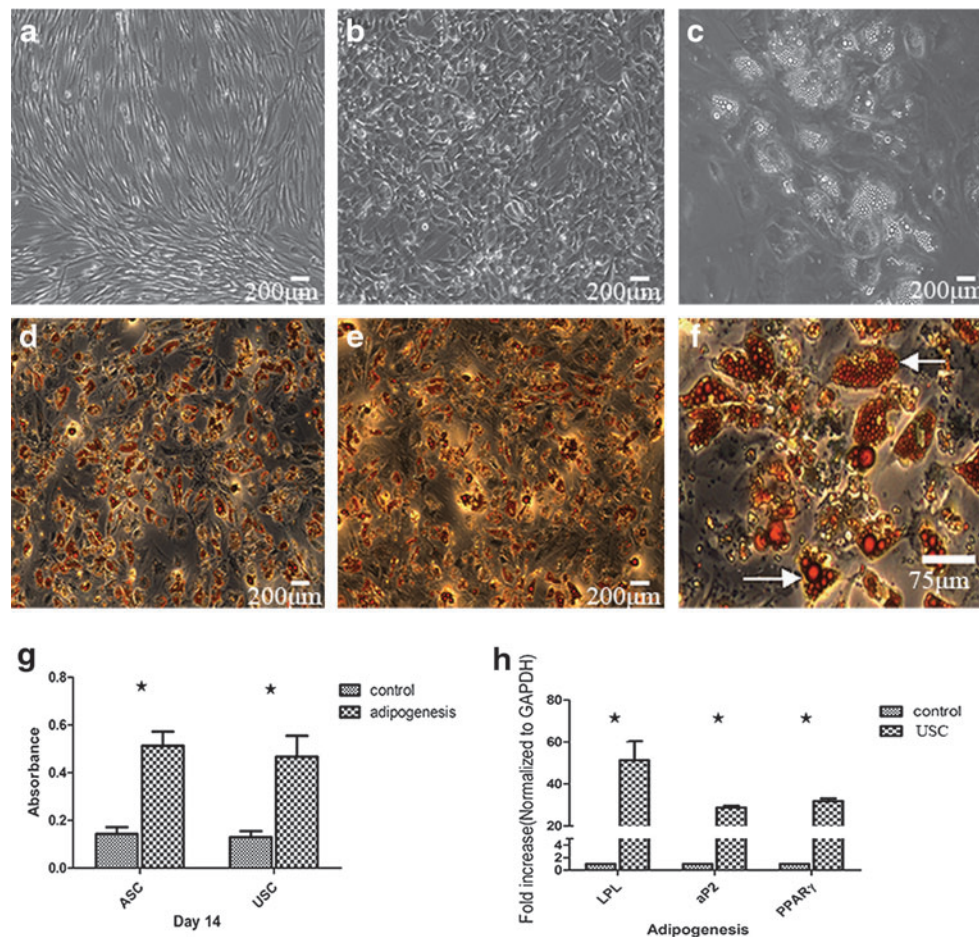


FIG. 4. Adipogenic differentiation results of USC and ASC. Before induction, USC represented spindle-shaped morphology (a). After 1 week of adipogenic induction, USC lost their spindle-shaped morphology and transformed into oblate morphology (b). After 2 weeks of induction, multisized and tiny intracytoplasmic lipid droplets were observed in USC under inverted phase-contrast microscope (c). Adipogenic differentiation of USC and ASC was demonstrated by Oil Red O staining (USCs: d; ASCs: e). When differentiation ended, the lipid droplets scattered around the cytoplasm of USC; some of them united to form larger ones (white arrow) (f). Quantitative measurements of lipid droplets through measured lipid droplets combined Oil Red O (g). Quantitative reverse-transcriptase-polymerase chain reaction (RT-PCR) results for lipoprotein lipase (LPL), ap2, and PPAR- γ (h, \star indicates significant difference of $p < 0.01$). All the images were taken under phase-contrast microscopy. Color images available online at www.liebertpub.com/tea

brain. These results demonstrated that USC exhibit a phenotype that is strikingly similar to ASC and represent an alternative cell source for neural tissue engineering.

Adult stem cells were first isolated from bone marrow and after that they have also been identified in multiple human tissues, including skeletal muscle, adipose tissue, cord blood, skin, dental pulp, and endometrium.^{23–28} It seems that every tissue possesses progenitor cells that play critical roles in tissue homeostasis and regeneration. Recently, urine was reported to contain viable cell types with stem cell characteristics.^{1,2,5} Testing with a large panel of cell markers, we demonstrated that USC display similar surface antigens to that of ASC. Previous study showed that USC could differentiate into urothelial, smooth muscle, and endothelial lineages.¹ Very recently Bharadwaj *et al.* reported that USC could differentiate into multilineage when cultured with appropriate differentiation medium.⁵ However, the intrinsic properties of USC still need further investi-

gation. Our results showed that USC are able to differentiate into osteocytes, adipocytes, and chondrocytes, which is the cardinal feature of MSCs. These results demonstrated that USC adhere rigidly to the criteria of MSCs, proposed by the International Society of Cellular Therapy, and exhibit the following properties: great proliferative capacity, multilineage differentiation potential, and with specific cell surface markers.²⁰

ASC were first reported in 2002 by Zuk *et al.*²⁴ After that ASC were extensively applied in basic research and clinical treatment.⁶ In this study, the biological characteristics of USC were investigated and compared with ASC. The proliferation ability of USC is similar with that of ASC. USC also express similar pattern of surface antigens with that of ASC, although the percentage of certain antigens was different. Similar to ASC, USC had mesoderm differentiation ability. All these data demonstrated that USC exhibited similar biological properties with ASC. As USC

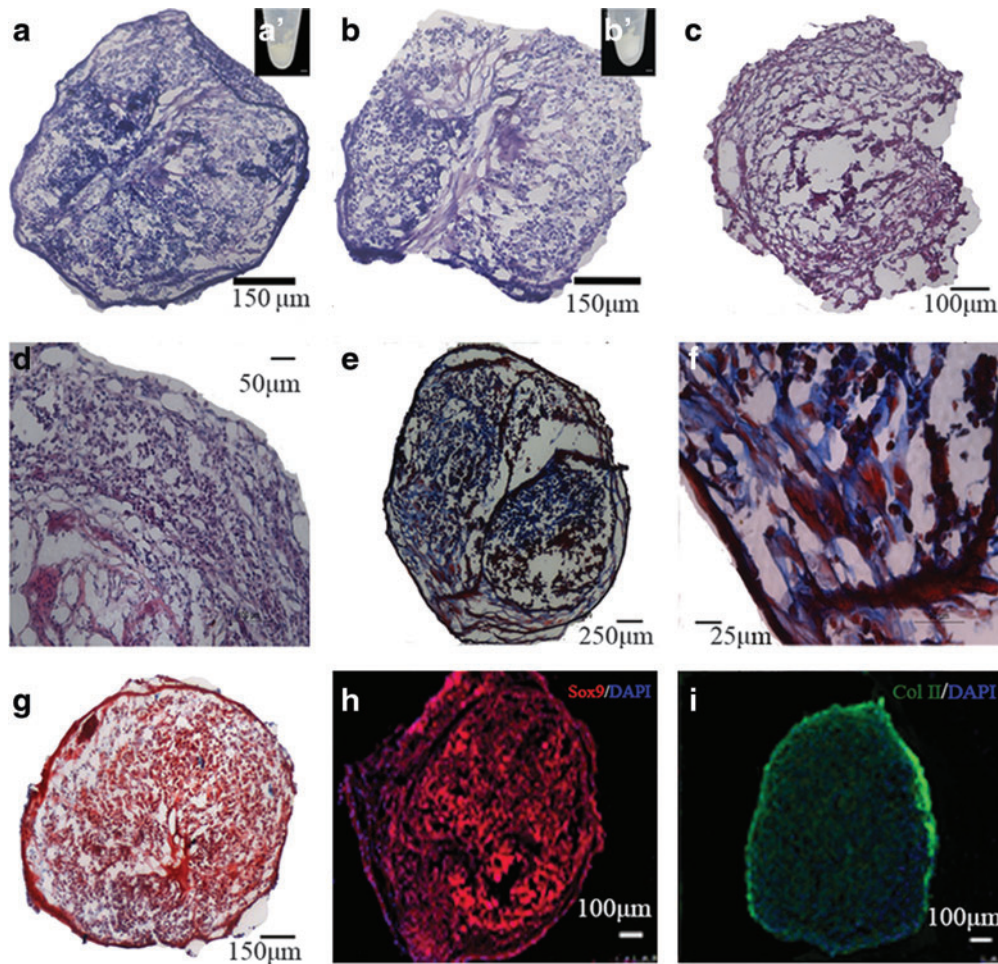


FIG. 5. Chondrogenic differentiation results of USC and ASC in the pellet culture system. Detection of polysaccharide extracellular matrix by toluidin blue staining (**a**: USC; **b**: ASC). After 4 weeks of induction, both USC and ASC formed a shiny surface (USC: **a'**; ASC: **b'**). The pellets in USC group were further stained with hematoxylin and eosin (H&E) (**c**, **d**), Masson trichrome (**e**, **f**), and Safranin-O/fast green staining (**g**). Immunofluorescence detected chondrogenic-related proteins Sox9 and collagen II (**h**, **i**). Color images available online at www.liebertpub.com/tea

can be harvested from voided urine by a noninvasive procedure, they represent a desirable cell source for regenerative medicine.

Since USC were newly identified adult stem cells, the suitable culture medium for USC is still under investigation. Zhang *et al.* employed keratinocyte serum-free medium (KSFM) and progenitor cell medium in a 1:1 ratio.¹ In their follow-up study they utilized mixed medium composed of KSFM and embryonic fibroblast medium (EFM) in a 1:1 ratio.^{2,3,29,30} With KSFM and EFM medium in 1:1 ration, we obtained two kinds of cells: elongated and endothelial-like cells (Supplementary Fig. S1; Supplementary Data are available online at www.liebertpub.com/tea). To obtain a more purified cells, we adopted a new culture medium. Our culture medium contains a large number of growth factors: hEGF, PDGF, bFGF, and TGF- β , which are essential for adult stem cells. Meanwhile, we also added some hormones to promote the proliferation of USC. Our results demonstrated that the modified medium can facilitate cell adhesion and proliferation. Most importantly,

cells cultured in our medium showed uniform elongated morphology. The appraisal results implied that fibroblast-like cells possessed similar biological characteristics with ASC.

In this study, we directly injected undifferentiated USC into rat brain. Interestingly, immunofluorescence showed that the transplanted cells were positive for neuronal markers 3 weeks postsurgery. The positive staining demonstrated that the lesion site can promote USC to differentiate into neuronal lineage cells. It is well-known that self-repair mechanism would be activated after brain injury.³¹ On the other hand, the transplanted stem cells have the ability to promote neuronal regeneration and suppress inflammatory reaction. For example, bone-marrow-derived MSCs (BMSCs) stimulated by supernatant from rat brain lesion secret brain-derived neurotrophic factor, nerve growth factor, and vascular endothelial growth factor. Those factors can prevent the secondary lesion and enhance the self-repair ability.³² Whether USC have similar ability with BMSCs needs further investigation. We inferred that under the self-repair mechanism and the effect of transplanted stem cells,

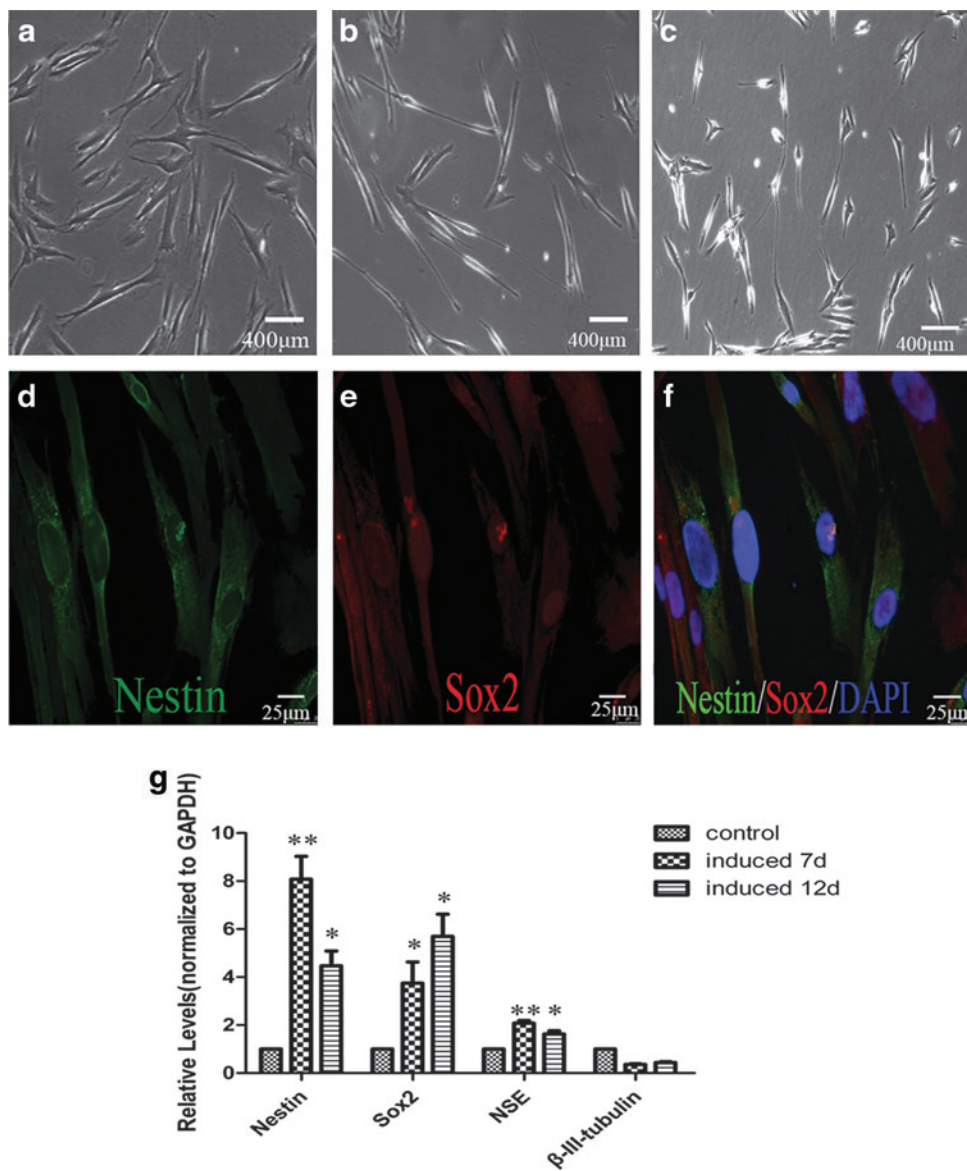


FIG. 6. *In vitro* neural differentiation results of USC. Morphology of undifferentiated USCs (a), 7 days (b) and 12 days (c) after exposure to the neural differentiation medium. Quantitative RT-PCR analysis of neural markers in neural-like cells at the days 7 and 12 showed that the expression of (d) Nestin, (e) Sox2, (f) and NSE notably increased compared with undifferentiated counterpart (g, * $p < 0.05$; ** $p < 0.01$). The expression level of β -III-tubulin did not change significantly. Color images available online at www.liebertpub.com/tea

the local microenvironment would modulate the behavior of USC and promote their differentiation into neuronal lineage cells. Santiago *et al.* transplanted undifferentiated ASCs into rat sciatic nerve defect. Full regeneration was achieved in ASC group, while no regeneration was occurred in the defect that was left empty. The author regarded that the transplanted stem cells release factors and support neurite outgrowth.³³ However, ASCs did not differentiate into neural lineage cells. The detailed reasons for different results between our research and Santiago investigation were elusive, but the different repair mechanisms between central and peripheral nervous system may play a critical role.³¹

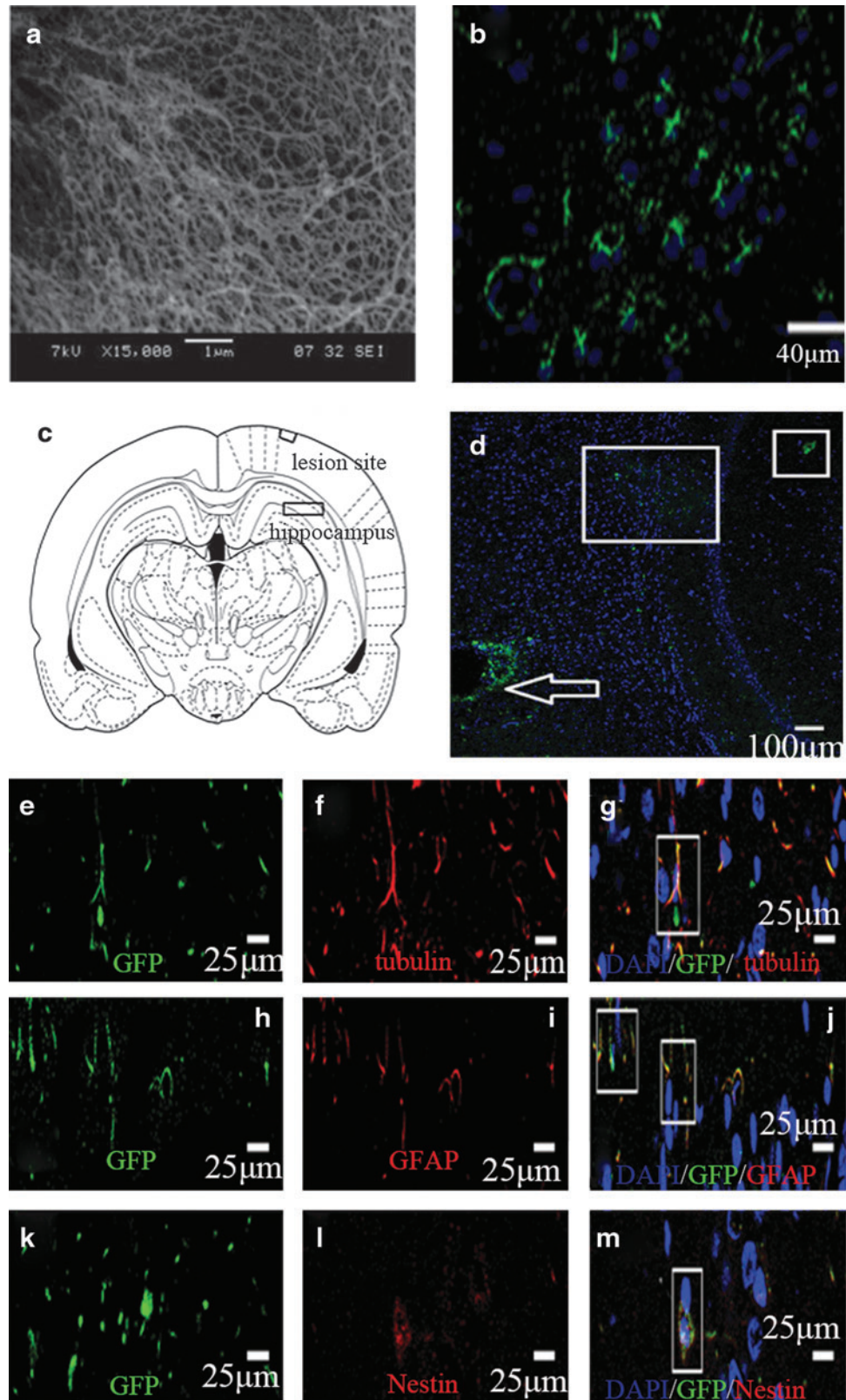
The migration of transplanted cells is critical for tissue regeneration. When USC were transplanted into rat lesion site, they were found to migrate to hippocampus. Studies have proved that hippocampus is a critical site for neuron formation.³⁴ Although the migration process is complicated and involved many growth factors and signaling pathways,

we inferred that the migrated cells can integrate into and coordinate with the local neurons.

Hydrogel is widely regarded as ideal scaffold material to study cell functions, such as cell survival, differentiation, and migration.¹³ As for neural tissue engineering, the desirable scaffold should have suitable physical, chemical, and biological properties. BeaverNano hydrogel scaffolds mimic the natural extracellular matrix of brain tissue and have excellent biocompatibility. The three-dimensional matrix provides a biomimic environment, which supports cell growth and tissue regeneration.

In summary, our data suggest that urine may contain a fraction of cells with stem cell characteristics. Surface antigen profile shows that USC have similar antigen marker to ASCs. Aside from their multilineage differentiation potentials, such as osteogenesis, adipogenesis, and chondrogenesis, USC can be successfully differentiated into neural lineage cells. After transplantation into rat brain, USC can survive,

FIG. 7. Green fluorescent protein (GFP)–USC survival, migration, and neural differentiation in rat brain. SEM image of the hydrogel showed the porous nature of the scaffold (**a**). Confocal image revealed large number of GFP-positive cells in the lesion site (**b**). Three weeks after transplantation, GFP-USCs migrated from the lesion to hippocampus (**c**: schematic diagram; **d**: white arrow: lesion site, rectangle: hippocampus). Immunofluorescence revealed the transplanted GFP-positive USCs existed within and around the lesion site (**e**, **h**, and **k**). The GFP-USCs were positive for β -III-tubulin (**f**, **g**: rectangle showed GFP and β -III-tubulin coexpressed cells), glial fibrillary acidic protein (GFAP) (**i**, **j**: rectangle showed GFP and GFAP coexpressed cells), and nestin (**l**, **m**: rectangle showed GFP and nestin coexpressed cells). Color images available online at www.liebertpub.com/tea



migrate, and differentiate in brain tissue. These data, together with previous work, strongly support that USCs have a similar biological characteristic with ASCs. The simplicity of isolation method and abundant sources of urine make USCs very attractive for tissue engineering and cytototherapy.

Acknowledgments

This work was supported by the National High Technology Research and Development Program of China (2012AA020506) and National Nature Science Foundation Grants (81160154 and 81060324).

Disclosure Statement

No competing financial interests exist.

References

- Zhang, Y., McNeill, E., Tian, H., Soker, S., Andersson, K.E., Yoo, J.J., *et al.* Urine derived cells are a potential source for urological tissue reconstruction. *J Urol* **180**, 2226, 2008.
- Bharadwaj, S., Liu, G., Shi, Y., Markert, C., Andersson, K.E., Atala, A., *et al.* Characterization of urine-derived stem cells obtained from upper urinary tract for use in cell-based urological tissue engineering. *Tissue Eng Part A* **17**, 2123, 2011.
- Bodin, A., Bharadwaj, S., Wu, S., Gatenholm, P., Atala, A., and Zhang, Y. Tissue-engineered conduit using urine-derived stem cells seeded bacterial cellulose polymer in urinary reconstruction and diversion. *Biomaterials* **31**, 8889, 2010.
- Wu, S., Liu, Y., Bharadwaj, S., Atala, A., and Zhang, Y. Human urine-derived stem cells seeded in a modified 3D porous small intestinal submucosa scaffold for urethral tissue engineering. *Biomaterials* **32**, 1317, 2011.
- Bharadwaj, S., Liu, G., Shi, Y., Wu, R., Yang, B., He, T., *et al.* Multi-potential differentiation of human urine-derived stem cells: potential for therapeutic applications in urology. *Stem Cells* **31**, 1840, 2013.
- Zuk, P.A. The adipose-derived stem cell: looking back and looking ahead. *Mol Biol Cell* **21**, 1783, 2010.
- Gimble, J.M., Katz, A.J., and Bunnell, B.A. Adipose-derived stem cells for regenerative medicine. *Circ Res* **100**, 1249, 2007.
- Zuk, P.A., Zhu, M., Mizuno, H., Huang, J., Futrell, J.W., Katz, A.J., *et al.* Multilineage cells from human adipose tissue: implications for cell-based therapies. *Tissue Eng* **7**, 211, 2001.
- Bible, E., Chau, D.Y.S., Alexander, M.R., Price, J., Shakesheff, K.M., and Modo, M. The support of neural stem cells transplanted into stroke-induced brain cavities by PLGA particles. *Biomaterials* **30**, 2985, 2009.
- Alper, J. Geron gets green light for human trial of ES cell-derived product. *Nat Biotech* **27**, 213, 2009.
- Frantz, S. Embryonic stem cell pioneer Geron exits field, cuts losses. *Nat Biotech* **30**, 12, 2012.
- Adams, A.M., Arruda, E.M., and Larkin, L.M. Use of adipose-derived stem cells to fabricate scaffoldless tissue-engineered neural conduits *in vitro*. *Neuroscience* **201**, 349, 2012.
- Nisbet, D.R., Crompton, K.E., Horne, M.K., Finkelstein, D.I., and Forsythe, J.S. Neural tissue engineering of the CNS using hydrogels. *J Biomed Mater Res Part B Appl Biomater* **87B**, 251, 2008.
- Valmikinathan, C.M., Mukhatyar, V.J., Jain, A., Karumbaiiah, L., Dasari, M., and Bellamkonda, R.V. Photocrosslinkable chitosan based hydrogels for neural tissue engineering. *Soft Matter* **8**, 1964, 2012.
- Song, A., Rane, A.A., and Christman, K.L. Antibacterial and cell-adhesive polypeptide and poly(ethylene glycol) hydrogel as a potential scaffold for wound healing. *Acta Biomater* **8**, 41, 2012.
- Schneider, A., Garlick, J.A., and Egles, C. Self-assembling peptide nanofiber scaffolds accelerate wound healing. *PLoS One* **3**, e1410, 2008.
- Hermann, A., Gastl, R., Liebau, S., Popa, M.O., Fiedler, J., Boehm, B.O., *et al.* Efficient generation of neural stem cell-like cells from adult human bone marrow stromal cells. *J Cell Sci* **117**, 4411, 2004.
- Ruan, D., Zhang, Y., Wang, D., Zhang, C., Wu, J., Wang, C., *et al.* Differentiation of human Wharton's jelly cells toward nucleus pulposus-like cells after coculture with nucleus pulposus cells *in vitro*. *Tissue Eng Part A* **18**, 167, 2012.
- Yasuda, H., Kuroda, S., Shichinohe, H., Kamei, S., Kawamura, R., and Iwasaki, Y. Effect of biodegradable fibrin scaffold on survival, migration, and differentiation of transplanted bone marrow stromal cells after cortical injury in rats. *J Neurosurg* **112**, 336, 2010.
- Dominici, M., Le Blanc, K., Mueller, I., Slaper-Cortenbach, I., Marini, F., Krause, D., *et al.* Minimal criteria for defining multipotent mesenchymal stromal cells. The International Society for Cellular Therapy position statement. *Cytotherapy* **8**, 315, 2006.
- Suuronen, E.J., Wong, S., Kapila, V., Waghay, G., Whitman, S.C., Mesana, T.G., *et al.* Generation of CD133+ cells from CD133- peripheral blood mononuclear cells and their properties. *Cardiovasc Res* **70**, 126, 2006.
- Seong, J.M., Kim, B.C., Park, J.H., Kwon, I.K., Mantalaris, A., and Hwang, Y.S. Stem cells in bone tissue engineering. *Biomed Mater* **5**, 062001, 2010.
- Miller, J.B., Schaefer, L., and Dominov, J.A. Seeking muscle stem cells. *Curr Top Dev Biol* **43**, 191, 1999.
- Zuk, P.A., Zhu, M., Ashjian, P., De Ugarte, D.A., Huang, J.I., Mizuno, H., *et al.* Human adipose tissue is a source of multipotent stem cells. *Mol Biol Cell* **13**, 4279, 2002.
- Bieback, K., and Kluter, H. Mesenchymal stromal cells from umbilical cord blood. *Curr Stem Cell Res Ther* **2**, 310, 2007.
- Vishnubalaji, R., Al-Nbaheen, M., Kadalmani, B., Aldahmash, A., and Ramesh, T. Skin-derived multipotent stromal cells—an archival for mesenchymal stem cells. *Cell Tissue Res* **350**, 1, 2012.
- Perry, B.C., Zhou, D., Wu, X., Yang, F.C., Byers, M.A., Chu, T.M., *et al.* Collection, cryopreservation, and characterization of human dental pulp-derived mesenchymal stem cells for banking and clinical use. *Tissue Eng Part C Methods* **14**, 149, 2008.
- Gargett, C.E., and Masuda, H. Adult stem cells in the endometrium. *Mol Hum Reprod* **16**, 818, 2010.
- Liu, G., Pareta, R.A., Wu, R., Shi, Y., Zhou, X., Liu, H., *et al.* Skeletal myogenic differentiation of urine-derived stem cells and angiogenesis using microbeads loaded with growth factors. *Biomaterials* **34**, 1311, 2013.
- Lang, R., Liu, G., Shi, Y., Bharadwaj, S., Leng, X., Zhou, X., *et al.* Self-renewal and differentiation capacity of urine-derived stem cells after urine preservation for 24 hours. *PLoS One* **8**, e53980, 2013.
- Horner, P.J., and Gage, F.H. Regenerating the damaged central nervous system. *Nature* **407**, 963, 2000.
- Kim, H.J., Lee, J.H., and Kim, S.H. Therapeutic effects of human mesenchymal stem cells on traumatic brain injury

- in rats: secretion of neurotrophic factors and inhibition of apoptosis. *J Neurotrauma* **27**, 131, 2010.
33. Santiago, L.Y., Clavijo-Alvarez, J., Brayfield, C., Rubin, J.P., and Marra, K.G. Delivery of adipose-derived precursor cells for peripheral nerve repair. *Cell Transplant* **18**, 145, 2009.
34. Spalding, K.L., Bergmann, O., Alkass, K., Bernard, S., Salehpour, M., Huttner Hagen, B., *et al.* Dynamics of hippocampal neurogenesis in adult humans. *Cell* **153**, 1219, 2013.

Address correspondence to:
Yang Wang, PhD
Department of Orthopedic Surgery
Shanghai Sixth People's Hospital
Shanghai Jiaotong University
600 Yishan Road
Shanghai 200233
China

E-mail: wangy63cn@126.com

Zhi-Feng Deng, MD, PhD
Department of Neurosurgery
Shanghai Sixth People's Hospital
Shanghai Jiaotong University
600 Yishan Road
Shanghai 200233
China

E-mail: dengzf63@126.com

Chang-Qing Zhang, MD, PhD
Department of Orthopedic Surgery
Shanghai Sixth People's Hospital
Shanghai Jiaotong University
600 Yishan Road
Shanghai 200233
China

E-mail: zhangcq@sjtu.edu.cn

Received: September 16, 2013

Accepted: January 2, 2014

Online Publication Date: May 15, 2014